

# Performance Analysis of Three Absorption Heat Pump Cycles, Full and Partial Loads Operations

B. Dehghan, T. Toppi, M. Aprile, M. Motta

**Abstract**—The environmental concerns related to global warming and ozone layer depletion along with the growing worldwide demand for heating and cooling have brought an increasing attention toward ecological and efficient Heating, Ventilation, and Air Conditioning (HVAC) systems. Furthermore, since space heating accounts for a considerable part of the European primary/final energy use, it has been identified as one of the sectors with the most challenging targets in energy use reduction. Heat pumps are commonly considered as a technology able to contribute to the achievement of the targets. Current research focuses on the full load operation and seasonal performance assessment of three gas-driven absorption heat pump cycles. To do this, investigations of the gas-driven air-source ammonia-water absorption heat pump systems for small-scale space heating applications are presented. For each of the presented cycles, both full-load under various temperature conditions and seasonal performances are predicted by means of numerical simulations. It has been considered that small capacity appliances are usually equipped with fixed geometry restrictors, meaning that the solution mass flow rate is driven by the pressure difference across the associated restrictor valve. Results show that gas utilization efficiency (GUE) of the cycles varies between 1.2 and 1.7 for both full and partial loads and vapor exchange (VX) cycle is found to achieve the highest efficiency. It is noticed that, for typical space heating applications, heat pumps operate over a wide range of capacities and thermal lifts. Thus, partially, the novelty introduced in the paper is the investigation based on a seasonal performance approach, following the method prescribed in a recent European standard (EN 12309). The overall result is a modest variation in the seasonal performance for analyzed cycles, from 1.427 (single-effect) to 1.493 (vapor-exchange).

**Keywords**—Absorption cycles, gas utilization efficiency, heat pump, seasonal performance, vapor exchange cycle.

## I. INTRODUCTION

NOWADAYS the fossil fuels scarcity and green gas emissions are one of the main challenges facing the world [1] and these issues have brought an increasing attention toward ecological and efficient HVAC systems. Heat pumps are commonly considered as a technology able to contribute to the achievement of the targets [2] and, while vapor compression heat pumps represent the optimal solution for new buildings with low-temperature emitters [3], gas heat pumps (GHP) are a promising technology for retrofitting the

heating systems of existing buildings [4], [5].

A detailed study on cycles suitable for ammonia-water absorption heat pump application was carried out by Phillips [6], who compared the double-effect, the resorber-augmented, the generator-absorber heat-exchange (GAX), the double-effect regenerative, the variable-effect and the two-stage GAX cycles for heat pumping purposes. Among those, the GAX cycle, first patented by Altenkirch and Tenckhoff [7], was considered as the most promising, thanks to its good combination of efficiency and simple layout. The main feature of the GAX cycle is the ability to bring the rich (in refrigerant) solution above the boiling point by recovering heat from the hottest section of the absorber. However, even if the GAX cycle proved good efficiency when implemented in a gas absorption heat pump (GAHP), several improvements have been proposed, with the purpose of improving its efficiency. Among these alternatives, worth to be mentioned are the branched-GAX and the VX cycles.

The purpose of the branched-GAX [8] is to increase the heat of absorption to match the higher heat of desorption typically found in the GAX cycle. Even if the branched-GAX cycle promised significantly higher performances than the GAX cycle [9], the actual performance resulted just slightly higher [10] or even lower [11].

By investigating the different published researches about absorption heat pump cycles it is clear that there are only few available documents related to VX cycle. With the VX cycle [12] an additional heat recovery is added to the GAX cycle, with the purpose of generating vapor which further enriches the rich solution. This gives several benefits, which result in a higher efficiency than the GAX cycle: The GAX temperature overlap increases, the need for rectification is reduced and the heat of desorption decreases, improving the match between the absorption and the desorption side of the GAX. Three possible embodiments have been identified for the VX cycle, based on the pressure level of the VX absorber and desorber. Moreover, for each embodiment, several different layouts are possible.

This paper aims at comparing the single effect (SE) cycle, the GAX cycle and the VX cycle for gas-fired air-sourced heat pump applications. The SE cycle has been chosen because of its simplicity, a relevant feature for heating devices, especially if of small capacity, where the cost is an issue as important as efficiency. The GAX cycle has been selected because, being considered as the most fitting cycle for the considered application, it is implemented on most of the commercial units currently on the market. For what concerns the VX, preliminary calculation confirmed that it represents a more promising option to improve the efficiency above the GAX

B. Dehghan is with the Department of Energy, Politecnico di Milano, 20156 Milano, Italy (phone: +39 0223993958; e-mail: babak.dehghan@polimi.it).

T. Toppi is with the Department of Energy, Politecnico di Milano, 20156 Milano, Italy (phone: +39 0223993964; e-mail: tommaso.toppi@polimi.it).

M. Aprile is with the Department of Energy, Politecnico di Milano, 20156 Milano, Italy (phone: +39 0223993865; e-mail: marcello.aprile@polimi.it).

M. Motta is with the Department of Energy, Politecnico di Milano, 20156 Milano, Italy (phone: +39 0223993818; e-mail: mario.motta@polimi.it).

than the branched-GAX.

## II. MODELLING STRATEGY

### A. Brief Description of SE, GAX and VX Cycles

In this part three GAHP cycles shown Fig. 1 are described and their specific features are discussed briefly.

The SE cycle is the most basic cycle which can be considered for GAHP applications as it just consists in adding a flue gas heat exchanger (FHX) to the classical SE cycle to lower the exhaust gas temperature and preheat hot water (Fig. 1 (a)). The cycle consists of direct fired generator (DFG) with internal solution heat recovery, tray columns (COL1 and COL2), rectifier (REC) for refrigerant purification, condenser (CON), absorber (ABS), evaporator (EVA), the recuperative heat exchangers include the solution heat exchanger (SHX) and refrigerant heat exchanger (RHX), solution pump, and refrigerant and solution restrictors. The absorber and condenser are connected in parallel and are coupled hydronically in series to the FHX.

The second investigated cycle is the GAX one. In the GAX cycle, due to the temperature overlap between absorber and generator, some heat of absorption can be recovered internally and delivered to the generator, resulting in a higher COP [13]. The practical implementation of the GAX concept consists in using a solution-cooled absorber (SCA) and a water-cooled absorber (WCA), as shown in Fig. 1 (b). In the SCA, the refrigerant vapor is partially absorbed by the poor solution coming from the generator, while the rich solution is preheated. Since dilution of ammonia vapor into the poor solution is not completely done in the SCA, the solution leaving the SCA (point 29) should be further cooled in WCA to complete the absorption process.

The third investigated cycle is the VX one which can be deployed according three embodiments and several variations within the same embodiment [4]. The resulting cycles differ in terms of cycle layout and complexity. Among them, a variation of the low-pressure embodiment, with the VX absorption and desorption processes taking place at an intermediate pressure between the high and low pressures, has been chosen. In particular, the selected layout is the one presented in Fig. 1 (c), which has the favorable features of requiring just two pumps and of being relatively simple to be implemented. This specific VX cycle is obtained modifying the GAX cycle to introduce an intermediate pressure level, where an additional heat recovery can take place. The solution leaving the low pressure absorber (LPA) is pumped to the intermediate system pressure across the pump, from 30 to 31 and finally is split in two streams. The first goes toward the VXA heat exchanger and is heated and partially evaporated by the heat of absorption released by the solution leaving the SCA (where refrigerant vapor mixes with the poor solution and is partially absorbed). The generated vapor is absorbed in the intermediate pressure absorber (IPA) by the second stream leaving the split, which is further enriched, while the liquid solution is recirculated through a restrictor at low pressure. The split ratio is defined as the fraction of solution split

towards the IPA [14]. Compared with the GAX, a VX cycle through the IPA operates with a higher concentration at the generator, which is an advantage of VX cycle because of the associated larger temperature overlapping at the SCA (i.e., the difference between the bubble point temperatures of the rich solution in point 4 and the poor solution in point 20) that is the main driver for refrigerant vapor generation through recovery of absorption heat. Moreover, a richer solution can reduce the need for external rectification in the partial condenser [12].

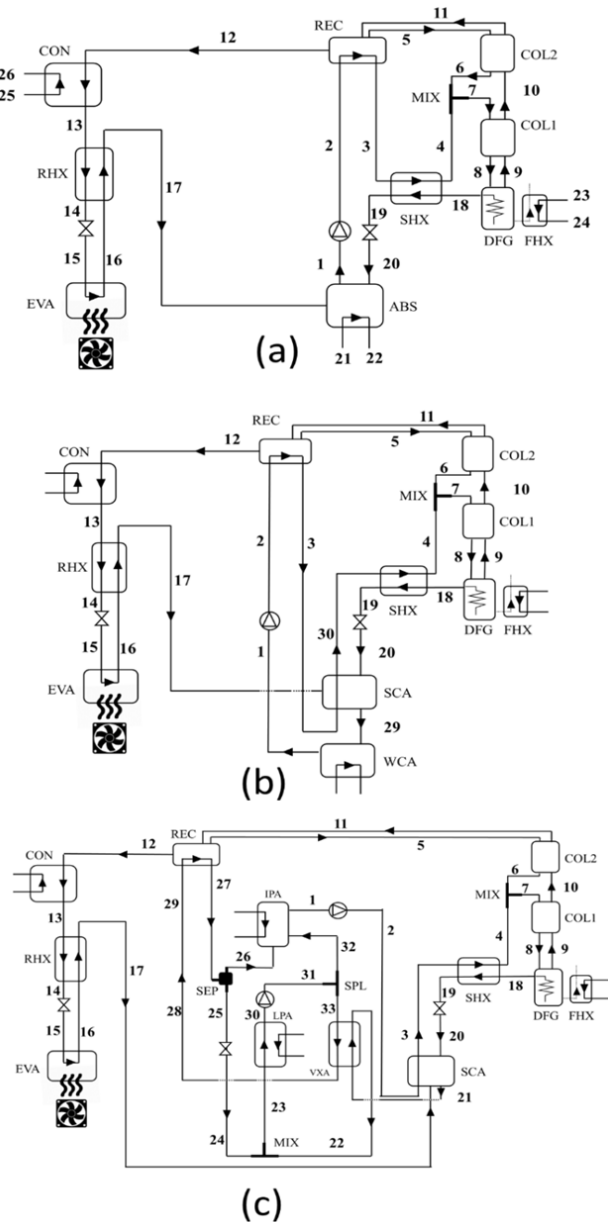


Fig. 1 Schematic of the investigated absorption cycles, (a) SE (b) GAX (c) VX

### B. Modelling Approach

The cycles described above were simulated using a modelling framework for steady-state simulation of absorption

cycles (STACY) [15]. This software is able to automatically name the different state points of cycles and build the set of equations, reducing programming time of advanced absorption heat pump (AHP) cycles and possible errors in setting a well-posed system of algebraic equations. The cycle modelling is based on a modular approach, which allows the definition of the mass, species and energy balances for each component volume exchanging mass through the associated ports ( $p = 1..N_p$ ).

$$\sum_{p=1}^{N_p} \dot{m}_p = 0 \quad (1)$$

$$\sum_{p=1}^{N_p} \dot{m}_p C_p = 0 \quad (2)$$

$$\sum_{p=1}^{N_p} \dot{m}_p h_p + Q_{in} + W_{in} = 0 \quad (3)$$

Additionally, conditions for the pressure levels of the cycle can be set, as well as additional conditions to close the system of equations. In particular:

- Sub-cooling or saturated liquid conditions are typically set at the outlet of generator, absorbers and condensers.
- Heat transfer is estimated based on  $\epsilon$ -NTU or approach temperature methods.
- The mass flow rate flowing through the restrictor of the solution is set as  $k\sqrt{\rho\Delta P}$ . Current operation setting reproduces the behavior of a real appliance containing a fixed restrictor with good accuracy (a typical solution in small size appliances), until the outlet is in liquid phase. The coefficient  $k$  has been tuned for each cycle in order to achieve 200 °C at the bottom of the generator at full load and at the highest thermal lift, i.e.  $T_{w,in} = 50$  °C,  $T_a = -10$  °C. With a fixed restrictor, at lower thermal lifts and at partial loads the temperature in the generator decreases and so the efficiency, especially for advanced cycles with high internal heat recovery (GAX, VX).

To obtain a realistic estimate of the partial load behavior of the cycles, the correct sizing of the heat exchangers and ways to estimate their thermal performance at varying loads are keys. Previous experiences [15], [16] on small size appliances have shown that fixed temperature approach or constant effectiveness can be set in most of the heat exchangers, especially condenser and evaporator. However, absorbers and internal heat recovery heat exchangers, namely SHX (for SE, GAX and VX cycles), ABS, WCA, SCA (for GAX and VX cycles), VXA, IPA, and LPA, are the most critical components and their off-design behavior has been carefully assessed. Plate heat exchangers are selected for the three SHX, the VXA and different water-cooled absorbers (ABS, WCA, LPA, IPA). Their performances can be calculated using the classical  $\epsilon$ -NTU expression for counter flow arrangement, in which the UA value is sized at the selected design condition (full load, evaporation temperature 0 °C and  $T_{w,in}$  40 °C) through an iterative approach until the target effectiveness or approach temperature is achieved. The results of this procedure are shown in Table I. Moreover, their off-design behavior is

predicted by correcting each partial UA value according to the 0.8 power of the related mass velocity.

TABLE I  
DESIGN PARAMETERS OF PLATE HEAT EXCHANGERS

HX	Cold side inlet mass (kg/h)	Hot side inlet mass (kg/h)	Target Value	Heat transfer rate (kW)	UA <sub>0</sub> (kW/K)
SHX (SE)	46.3	33.5	$\epsilon_0=0.85$	1.70	0.13
SHX (GAX)	51.2	34.7	$\epsilon_0=0.80$	0.50	0.10
SHX (VX)	49.0	31.5	$\epsilon_0=0.80$	0.44	0.09
ABS	656.9	33.5	$\Delta T_{min}=2K$	7.08	0.20
WCA	750.0	51.2	$\Delta T_{min}=4K$	8.12	0.70
LPA	651.2	95.95	$\Delta T_{min}=2K$	5.98	0.77
IPA	557.0	44.63	$\Delta T_{min}=2K$	2.02	0.50
VXA	49.3	49.03	$\epsilon_0=0.80$	2.25	0.25

The two SCA are in-tube vertical falling film absorber with gas and falling film in counter-current flow arrangement. The sizing of these components and their performances at the various loads are calculated by means of a validated numerical model, whose details can be found in [16]. The geometry and the operating conditions at design point for the GAX cycle are reported in Table II. The same heat exchanger geometry is used also in the VX cycle.

TABLE II  
DESIGN PARAMETERS OF SCA HEAT EXCHANGER (GAX CYCLE)

Parameter	Value	Unit
Tube internal diameter	13.8	mm
Tube external diameter	15.8	mm
Tube length	1000	mm
Number of tubes	19	-
Shell internal diameter	79.3	mm
Rich solution flow rate	51.2	kg/h
Poor solution flow rate	34.7	kg/h
Heat duty	2.28	kW

To be able to compare performance of SE, GAX and VX cycles, heating Gas Utilization Efficiency ( $GUE_h$ ) is defined as the ratio of the energy supplied by GAHP (i.e. heat transferred to the space heating system) to the energy input with the natural gas.

$$GUE_h = \frac{Q_{ex,con} + Q_{ex,abs} + Q_{hcf,DFG}}{Q_{gas,DFG}} \quad (4)$$

where  $Q_{ex,con}$  is the heat transfer rate of condenser,  $Q_{ex,abs}$  is heat transfer rate from solution to coolant.  $Q_{ex,DFG}$  is heat transfer rate from gas burner to boiling solution. Also  $Q_{hcf,DFG}$  and  $Q_{gas,DFG}$  are heat transfer rate from flue gas to heat carrier fluid and actual gas input [kW] respectively [15].

### III. SIMULATION RESULTS AND ANALYSES

#### A. Full Load Operation

In this section full load performance of GAHP system is investigated for three different cycles and results are presented respectively.

Fig. 2 (a) shows the plots of SE cycle  $GUE_h$  value versus

water temperatures for three different ambient cases. The  $GUE_h$  varies from 1.22 to 1.50 for the full range of water and ambient temperatures investigated. Referring to Fig. 2 (a),  $GUE_h$  value decreases as water temperature increases and SE cycle shows better performance in the case of high air temperatures as expected. Higher ambient temperatures let more heat to be transferred in the evaporator due to the greater driving temperature difference between the ambient and refrigerant streams. Lower water temperatures allow for more refrigerant to be generated due to the higher solution concentrations. As shown in Fig. 2 (b), higher efficiencies are linked to higher concentration of the rich solution. At low water temperatures, concentration of rich solution is high while it also increases with ambient temperature due to the higher pressure and temperature in evaporator.

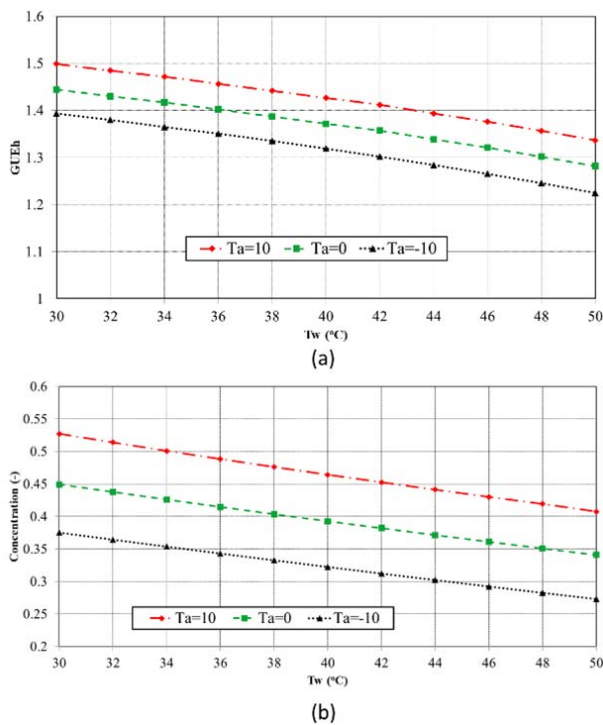


Fig. 2 (a) Full load performance of SE cycle,  $GUE_h$  (b) Concentration variations of the rich solution

Fig. 3 illustrates the simulation results of the GAX cycle. Based on investigations shown in Fig. 3 (a),  $GUE_h$  increases significantly below 34, 38 and 44 °C water temperatures respected to -10, 0 and 10 °C air temperatures due to the presence of vapor in the coolant side of the SHX heat exchanger. No vapor exists in exit stream of SHX when water temperatures are higher than 34, 38 and 44 °C while air temperatures are -10, 0 and 10 °C respectively due to the lower heat recovery. The  $GUE_h$  achieved by the GAX cycle is in the range 1.25-1.67, which is higher than the SE cycle. The increase in performance is explained by the GAX effect [17], i.e. the ability of desorbing part of refrigerant by recovering part of the released heat in absorber and it takes place when the thermal lift is sufficiently low. In particular, expressing the

GAX effect in terms of vapor quality in the rich solution after the SHX, the trends represented in Fig. 3 (b) are found. In Fig. 3 (b), the GAX effect is displayed in terms of vapor quality of rich solution after SHX and, as it is shown, increment in ambient air temperature and reduction in water temperature allow for more vapor to be generated. As water temperature rises, the high pressure increases, while the low pressure is limited by the external temperatures at the evaporator and consequently, GAX effect first decreases and then completely disappears. As discussed earlier, at full load and with increasing hot water temperatures,  $GUE_h$  is decreased due to the lowering of the concentration spread and the resulting loss in effectiveness of the internal heat recovery between the desorption and the absorption processes and consequently, GAX effect vanishes with hot water temperature of 50 °C and ambient air temperatures of -10 °C (no vapor in these conditions).

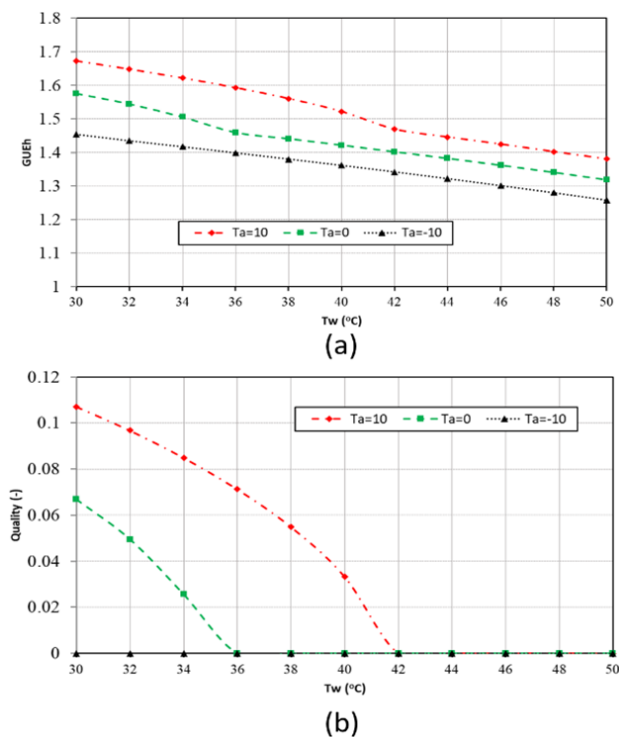
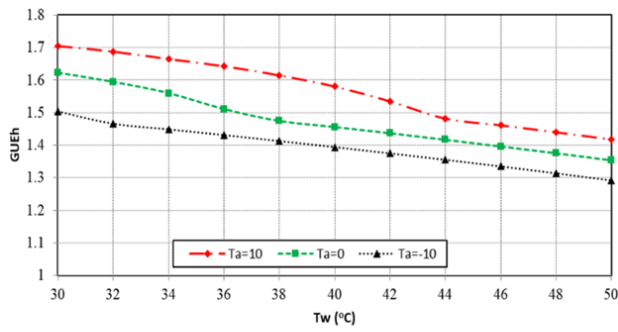


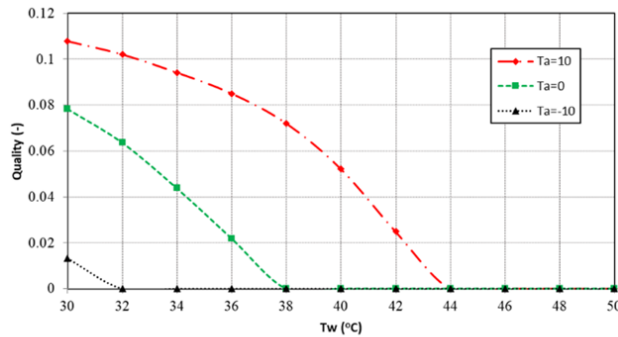
Fig. 3 (a) Full load performance of GAX cycle,  $GUE_h$  (b) vapor quality of solution at the exit of SHX

Final simulated cycle is VX one. The GAX cycle which is employed in most of the commercial heat pumps is modified to introduce the VX concept which is following same principle of GAX cycle. This fact will enable higher mass fraction in the rich solution. In this cycle, the split ratio is defined as the fraction of solution split towards the LPA [14]. Fig. 4 (a) shows maximum possible  $GUE_h$  values versus different water temperature ranging 30-50 °C for three different air temperatures (-10, 0, 10 °C). As it is shown, GUE covers range of 1.3-1.7 for VX cycle which is higher than that of GAX and SE.

Results show that, because of the vapor generation in the coolant side of the SHX (as shown in Fig. 4 (b)) due to the heat recovery in it,  $GUE_h$  and  $COP_h$  increase significantly below 32, 38 and 44 °C water temperatures when air temperatures are -10, 0 and 10 °C respectively. As it was discussed, in a VX cycle, an extra heat recovery is added to the GAX cycle, with the purpose of generating vapor which further enriches the rich solution and consequently, improves GAX effect. In Fig. 4 (b) vapor quality of the rich solution at the exit of SHX is indicated. Comparison between VX and GAX results manifests the effectiveness of VX cycle and it shows that in the VX cycle more heat between desorber and absorber can be recovered and consequently more vapor can be generated in the coolant side of the SHX even in high thermal lifts. Unlike GAX cycle, in VX one, GAX effect appears when ambient air temperature is -10 °C.



(a)



(b)

Fig. 4 (a) Full load performance of GAX cycle,  $GUE_h$  (b) vapor quality of solution at the exit of SHX

Based on the presented results, among the analyzed cycles, the VX one is found to achieve the highest GUE which is approximately 11.3% and 3.3% higher than SE and GAX performances regarding to water temperatures less than 34 °C (keeping ambient air temperature constant 0 °C).

### B. Seasonal Performance

In this part seasonal performance of GAHP is investigated for three mentioned cycles at reduced gas input loads according to European standard [18]. The standard proposes

the calculation for three different climates (cold, average and warm) with design temperature of -22 °C, -10 °C and 2 °C. Moreover, four applications are considered, namely very high temperature, high temperature, medium temperature and low temperature applications, characterized by nominal water supply temperatures of 65 °C, 55 °C, 45 °C and 35 °C. In this work, the high temperature application in the average climate is considered for the calculations. When an appliance undergoes performance certification, the GUE is measured at the conditions reported in Table III.

TABLE III  
PART LOAD WORKING CONDITIONS

Operation number	Part load ratio (PLRh)	Tair dry bulb (°C)	Tw, in (°C)	Tw, out (°C)
1	100%	-10	41.3	55.0
2	88%	-7	39.3	52.0
3	54%	2	32.7	42.0
4	35%	7	28.7	36.0
5	15%	12	24.7	30.0

Based on the bin method, the seasonal heating gas utilization efficiency ( $SGUE_h$ ) is defined as the ratio of the overall heating energy to the overall gas consumption;

$$SGUE_h = \frac{\sum_{j=1}^n h_j \times Q_h(T_j)}{\sum_{j=1}^n h_j \times \left( \frac{Q_h(T_j)}{GUE_h(T_j)} \right)} \quad (5)$$

where  $T_j$  is the bin temperature,  $j$  is bin number,  $n$  is the number of bins,  $Q_h(T_j)$  is the heating load of the building for the corresponding temperature  $T_j$  expressed in kW,  $h_j$  is the number of bin hours occurring at the corresponding temperature  $T_j$ ,  $GUE_h(T_j)$  is GUE at the corresponding temperature  $T_j$ . The values to be used for  $j$ ,  $T_j$ , and  $h_j$  are determined based on EN12309-6 standard [18].

To investigate seasonal performance of SE, GAX and VX cycles, partial load operating conditions given in Table III are applied and  $GUE_h$  values are calculated from simulation results. Also required heating load  $Q_h$  is determined by:

$$Q_h = Q_{ex,con} + Q_{ex,abs} + Q_{hcf,DFG} \quad (6)$$

The results of the numerical simulation for the three cycles and related to the five operating conditions are reported in Tables IV- VI. In particular, for each condition can be found the heating capacity, the gas input and the resulting GUE values, which are used for the calculation of the SGUE for each cycle. Moreover, in order to provide a better insight on the cycles' behavior, the mass fraction of the rich and poor solution and the maximum generator temperature are also given.

Values of 1.427, 1.452 and 1.493 are found for SE, GAX and VX respectively. The differences among the cycles are smaller than the difference found at full load. This can be explained by looking at the temperature of the solution at the bottom of the generator ( $T_b$ ), which drops significantly moving from condition #1 to condition #5. The drop in

temperature is explained by the combination of a lower thermal lift, which gives higher mass fraction of the rich solution, and of a lower thermal input. The generator temperature reduction causes an increase of the poor solution mass fraction, which leads to an increasingly smaller concentration spread and to a higher circulation ratio, both detrimental for the efficiency. This is particularly evident in condition #5, where the GAX cycle is behind cut-off, while the SE and the VX operate with a mass fraction difference between rich and poor solution of about 5%. Moreover, by increasing the mass fraction of the poor solution, the GAX effect in both the GAX and VX cycles decreases and disappears for all operating conditions (#1 to #5), which experience a larger efficiency reduction compared to the full load operation. It is important to mention that, with a sharp drop in temperature of the solution at the bottom of generator ( $T_b$ ) which dissipates a fraction of the heat recovery potential, the GAX effect vanishes at partial loads.

TABLE IV  
SEASONAL PERFORMANCE OF SE CYCLE

Operation number	$Q_h$ (kW)	GUE	$Q_{gas,nom}$ (kW)	$T_b$	$C_{poor}$	$C_{rich}$	$SGUE_h$
1	13.0	1.300	10.00	200.0	0.088	0.314	1.427
2	11.44	1.327	8.62	182.0	0.140	0.346	
3	7.02	1.418	4.95	127.1	0.308	0.448	
4	4.58	1.478	3.10	95.8	0.415	0.512	
5	1.95	1.488	1.31	65.4	0.543	0.585	

TABLE V  
SEASONAL PERFORMANCE OF GAX CYCLE

Operation number	$Q_h$ (kW)	GUE	$Q_{gas,nom}$ (kW)	$T_b$	$C_{poor}$	$C_{rich}$	$SGUE_h$
1	13.24	1.324	10.00	200.0	0.071	0.308	1.452
2	11.65	1.359	8.57	179.9	0.129	0.345	
3	7.15	1.474	4.85	121.6	0.315	0.462	
4	4.63	1.523	3.04	89.4	0.434	0.535	
5	-	1.327	-	-	-	-	

TABLE VI  
SEASONAL PERFORMANCE OF VX CYCLE

Operation number	$Q_h$ (kW)	GUE	$Q_{gas,nom}$ (kW)	$T_b$	$C_{poor}$	$C_{rich}$	$SGUE_h$
1	13.64	1.364	10.00	200.0	0.070	0.357	1.493
2	12.00	1.395	8.60	180.8	0.126	0.385	
3	7.36	1.493	4.93	125.2	0.298	0.474	
4	4.77	1.539	3.10	94.7	0.407	0.529	
5	2.04	1.545	1.32	66.5	0.526	0.581	

#### IV. CONCLUSION

Full load operation (100% gas input) confirmed that the lowest performances are achieved by the SE cycle and that higher efficiency is obtained with the GAX and VX cycles. In particular, varying the air temperature from -10 °C to 10 °C and the inlet water temperature from 30 to 50 °C the GUE varies between 1.22-1.50, 1.25-1.67, 1.30-1.70 corresponding to SE, GAX and VX cycles. Moreover, the benefit of the GAX effect, obtained thanks to vapor generation by means of internal recovery in the SCA and SHX, increase at low thermal lifts, i.e. at high air temperature and low return water

temperature, while it firstly decreases and then disappears as the lift becomes higher. The benefits of the GAX effect are further amplified in the VX cycle, because of a higher concentration in the rich solution, which eases the vapor generation and extends the temperature range where it can be achieved. Those differences in terms of performances among the cycles are less evident in the seasonal performances calculation. In fact, in heat pump mode the cycles operate either at high thermal lift or at low gas input, conditions that reduce the GAX effect. In fact, when the gas input is lowered, the generator temperature decreases, the poor solution concentration increases and the temperature overlap required for the GAX effect disappears. Although higher performance changes are expected as thermal lift decreases, the magnitude of this increase is lowered due to the reduction of gas input power which negatively affects GUE. Therefore, as results show, the GUE value is increased slightly while thermal lift decreases. These results suggest that for heat pump application the SE or the GAX cycles are the most suitable because their simpler layout overcompensate the slightly lower performance. It is expected that using the variable restrictor to modulate the poor solution flow rate may increase the SGUE for all the cycle, especially for the GAX and the VX. In this case, the larger performance gap could improve the attractiveness of the VX cycle, even considering the more complex layout.

#### REFERENCES

- [1] M. Toub, C.R. Reddy, M. Razmara, M. Shahbakhti, R.D. Robinett, G. Aniba. Model-based predictive control for optimal MicroCSP operation integrated with building HVAC systems. *Energy Conversion and Management*. 199 (2019) 111924.
- [2] B. Dehghan B. L. Wang, M. Motta, N. Karimi. Modelling of waste heat recovery of a biomass combustion plant through ground source heat pumps- development of an efficient numerical framework. *Applied Thermal Engineering*. (2019) 114625.
- [3] G. Kosmadakis. Estimating the potential of industrial (high-temperature) heat pumps for exploiting waste heat in EU industries. *Applied Thermal Engineering*. 156 (2019) 287-98.
- [4] R. Scoccia, T. Toppi, M. Aprile, M. Motta. Absorption and compression heat pump systems for space heating and DHW in European buildings: Energy, environmental and economic analysis. *Journal of Building Engineering*. 16 (2018) 94-105.
- [5] T. Jia, E. Dai, Y. Dai. Thermodynamic analysis and optimization of a balanced-type single-stage NH<sub>3</sub>-H<sub>2</sub>O absorption-desorption heat pump cycle for residential heating application. *Energy*. 171 (2019) 120-34.
- [6] B.A. Phillips. Development of a High-Efficiency. Gas-fired. Absorption Heat Pump for Residential and small-commercial applications. Phase I Final Report Analysis of Advanced Cycles and Selection of the Preferred Cycle 1990.
- [7] T.B. Altenkirch E. Absorptionskaeltemaschine zur kontinuierlichen erzeugung von kaelte und waerme oder auch von arbiel. German Patent 278076. (1914).
- [8] Donald C. Erickson, S. Harbor, M. Annapolis. Branched GAX Absorption Vapor Compressor. In: U.S. Patent, (Ed.). United States, 1991.
- [9] K. Herold, H. Xiaoyu, D. Erickson, M. Rane. The branched GAX absorption heat pump cycle. *Jpn Assoc Refrig Abs Heat Pump Conf*. (1991) 27-33.
- [10] M. Engler, G. Grossman, H.M. Hellmann. Comparative simulation and investigation of ammonia-water: absorption cycles for heat pump applications. *International Journal of Refrigeration*. 20 (1997) 504-16.
- [11] Donald C. Erickson, G. Anand, A. Riyaz. Branched GAX Cycle Gas Fired Heat Pump. *Energy Concepts Co*. (1996).
- [12] D.C. Erickson. Vapor Exchange Duplex GAX Absorption Cycle. United States Patent 5 097 676. (1992).

- [13] E. Dai, M. Lin, J. Xia, Y. Dai. Experimental investigation on a GAX based absorption heat pump driven by hybrid liquefied petroleum gas and solar energy. *Solar Energy*. 169 (2018) 167-78.
- [14] M.A. Tommaso TOPPI, Marco GUERRA, Mario MOTTA. Incorporating the VX concept in a commercial GAX heat pump: a numerical study. *ISHPC2017*. (2017).
- [15] M. Aprile, T. Toppi, S. Garone, M. Motta. STACY–A mathematical modelling framework for steady-state simulation of absorption cycles. *International Journal of Refrigeration*. 88 (2018) 129-40.
- [16] M. Aminyavari, M. Aprile, L. Pistocchini, M. Motta. Modelling and experimental validation of an in-tube vertical falling film absorber with counter flow arrangement of solution and gas. *International Journal of Refrigeration*. 100 (2019) 72-82.
- [17] M. Aprile, R. Scoccia, T. Toppi, M. Guerra, M. Motta. Modelling and experimental analysis of a GAX NH<sub>3</sub>–H<sub>2</sub>O gas-driven absorption heat pump. *International Journal of Refrigeration*. 66 (2016) 145-55.
- [18] EN12309-6. Gas-fired sorption appliances for heating and/or cooling with a net heat input not exceeding 70 kW – Part 6: Calculation of Seasonal Performances. (2014).